Int. J. Electrochem. Sci., 10 **(2015)** 10597 - 10606

International Journal of
ELECTROCHEMICAL
SCIENCE
www.electrochemsci.org

Effects of Fibrous Nickel Additives on the Electrochemical Properties of $LiFePO_4$ Cathode for Lithium-ion Battery

Sheng-wen Zhu[1], *Mao-xiang Jing*[1,2,*], *Zhi-chao Pi*[1], *Li-li Chen*[1], *Xiang-qian Shen*[1,*]

[1] Institute for Advanced Materials Science, School of Materials Science and Engineering, Jiangsu University, Zhenjiang, China, 212013
[2] Jingjiang college, Jiangsu University, Zhenjiang, China, 212013
[*]E-mail: mxjing2004@mail.ujs.edu.cn, shenxq@ujs.edu.cn

Received: 28 September 2015 / *Accepted:* 26 October 2015 / *Published:* 4 November 2015

In this paper, the effects of fibrous nickel(Ni) additives on the electrochemical performance of $LiFePO_4$ as a lithium-ion battery cathode were investigated by a simple mixing process of $LiFePO_4$ powders and porous nickel fibers. The microstructure and crystalline phase were characterized by scanning electron microscopy (SEM) and X-ray diffractometry (XRD). The electrochemical properties of nickel fiber/$LiFePO_4$ composite were analyzed by the electrochemical impedance spectroscopy(EIS), cyclic voltammetry(CV), and galvanostatic charge/discharge test. Highly conductive Ni additive can enhance the electronic conductivity of $LiFePO_4$. Electrode fabricated from nickel fiber/$LiFePO_4$ composite as lithium-ion battery cathode exhibits better electrochemical performance compared with pristine $LiFePO_4$. The electrode with optimal fiber content of 10wt% has the best redox kinetics and possesses a good rate capability of 85 mAh g^{-1} even at 5C, versus 60 mAh g^{-1} for pristine $LiFePO_4$. It also shows good cyclability with initial discharge capacity of 131.1 mAh g^{-1} at 1C, and the retention capacity of 119.8 mAh g^{-1} after 100 cycles, whereas pristine $LiFePO_4$ only delivers 108.2 mAh g^{-1} at the same condition and retention capacity of 100.9 mAh g^{-1} after 100 cycles.

Keywords: Lithium-ion battery, $LiFePO_4$, Nickel fiber, Conductive additive, Mechanical mixing

1. INTRODUCTION

Olivine structured $LiFePO_4$ as a hopeful cathode material for lithium-ion battery (LIB) has drawn wide interests owing to its abundant and environmentally friendly sources and excellent safety[1-5]. However, its poor electronic conductivity and ionic conductivity between the $LiFePO_4$/$FePO_4$ interface could result in large initial capacity loss and poor rate capability[6-10].

Tremendous efforts have been made to overcome the inherent limitations of $LiFePO_4$ including combination with various kinds of conductive carbonaceous materials such as carbon powders[11], graphene[12], carbon nanotube(CNF)[13], etc. However, when these carbon-based conductive powders were added into the viscous $LiFePO_4$ slurry, the interconnection between conductive additives was demanded to fully percolate from a current collector surface to the outer-most active particle layer, and form long-range conductive networks. While this particle percolation with impalpable volumetric content demands conductive fillers with high specific surface area and uniform dispersion, which usually influence the battery performance and decrease the speed, yield, and cost of production [14].

Recently, three-dimensional bicontinuous composites have attracted much attention. Lang et al proposed a paradigm to manufacture high-rate rechargeable battery through the use of a three-dimensional bicontinuous composite electrode design, which can provide efficient and rapid transport pathways for ion and electron. The ultrafast rate performance demonstrated by the bicontinuous electrode provides an electrochemical storage technology with the power density of a supercapacitor and the energy density of a battery[15]. Hou et al also reported a three-dimensional bicontinuous nanoporous Cu/MnO_2 hybrid electrode, which demonstrates a high capacity of 1100 $mAhg^{-1}$ after 1000 cycles[16]. However, this concept can not be used to prepare $LiFePO_4$-based composite cathodes due to the complexity of the preparation process. Ahn et al fabricated metal fibers/$LiCoO_2$ composite electrode by using 316L stainless steel fiber with 1.5um in diameter and 0.1~2mm in length, and affirmed that there is minimal parasitic reactions, while the discharge capacity and cyclability were enhanced [14]. Whereas, it is worth to note that due to the rigid fibers with large aspect ratio, the optimal content of fibers appears less that 4.5wt% to avoid increasing the difficulty of slurry mixing and decreasing the electrode uniformity, meanwhile, the safety of the battery from this composite could be influenced as the possibility of piercing separator by rigid fibers increased.

In our group's recent work, we found that porous nickel(Ni) fibers with low aspect ratio as conductive additive and electrocatalyst could obviously improve the electrochemical performance of Li-S battery[17]. Could the electrochemical performance of $LiFePO_4$ cathode be improved by utilizing low aspect ratio Ni fibers as conductive additive? In this paper, we utilized low aspect ratio, micro-sized Ni fibers as conductive additive to prepare Ni/$LiFePO_4$ composite cathode by facile mixing process. The effects of Ni fibers on the electrochemical properties of $LiFePO_4$ were studied. Compared with pristine $LiFePO_4$ electrode, the electrodes containing nickel fibers showed an obviously improved cyclability and rate performance.

2. EXPERIMENTAL

2.1 Preparation and characterization of nickel fibers/$LiFePO_4$ composites

Nickel fibers were fabricated via a precipitation-thermal reduction method as described by the previous reports [18, 19]. In a typical synthesis, 100mL mixed solution of nickel chloride(1M) and oxalic acid(1M) was prepared firstly with 1:1 molar ratio. Then, 10ml polyvinylpyrrolidone (K30) solution with a concentration of 0.3wt% was added into the above solution, and the pH value was adjusted to 8.0 by ammonia solution. The fibrous precipitates were appeared when the mixed solution was mechanically stirred at 40~50ºC for 3h. Thereafter, the precipitates were filtrated and washed with

deionized water, ethanol, and acetone, respectively, then dried in air at 100ºC for 12h. Finally, the porous and low aspect ratio nickel fibers were obtained after the dried precipitates were thermal decomposed and reduced in a N_2 / H_2 mixed atmosphere with $V(N_2)$: $V(H_2)$~9:1 at 450ºC for 30 min.

$LiFePO_4$ nano powders were prepared by a hydrothermal route[20]. Firstly, 40mL mixed solution of LiH_2PO_4 (2mM) and $FeSO_4 \cdot 7H_2O$(2mM) was prepared. Then, 1 ml of ethylenediamine was slowly added into the above solution, stirring at room temperature, and forming a green brown clear solution. The mixed solution was transferred into a 50 ml Teflon-lined stainless steel autoclave and heated to 200ºC in an oven for 3h. When cooled to room temperature, the precipitates were filtrated and washed with deionized water, ethanol, and acetone respectively, then dried in a vacuum oven at 80 ºC for 12 h. The resultant products were obtained after the dried precipitates was crystallined in a tube furnace under Ar atmosphere at 600 ºC for 6 h.

Nickel fiber /$LiFePO_4$ composites with different nickel fiber content were prepared by simple mixing process of nickel fibers and $LiFePO_4$ powders using a agate mortar in absolute ethyl alcohol solution at the room temperature. After grinded, the composites were dried in a vacuum oven at 80 ºC for 12 h , and reserved in vacuum for the preparation of composite electrodes. The weight ratios of Nickel fiber /$LiFePO_4$ composites were listed in Table 1. The schematic representation of the electrode from nickel fibers/$LiFePO_4$ composites was shown in Fig.1, the $LiFePO_4$ powders are expressed by spheres for simplicity.

Table 1. The weight ratio of composite cathode material.

Sample	The weight ratio (%)	
	Nickel fibers loading	$LiFePO_4$ loading
$LiFePO_4$/Ni-0	0	80
$LiFePO_4$/Ni-1	0.8	79.2
$LiFePO_4$/Ni-5	4	76
$LiFePO_4$/Ni-10	8	72
$LiFePO_4$/Ni-20	16	64
$LiFePO_4$/Ni-30	24	56

The crystalline phases were measured on a Rigaku Smart Lab X-ray diffractometer at 40 kV using a Cu Kα radiation with a scanning rate of 6º min^{-1}. The morphology and microstructure of the nickel fibers and nickel fibers/$LiFePO_4$ composites were observed by scanning electron microscopy (SEM, JIM-7001F, Japan). The distribution of elements on the surface of nickel/$LiFePO_4$ composites were identified by energy-dispersive X-ray spectroscopy (EDS).

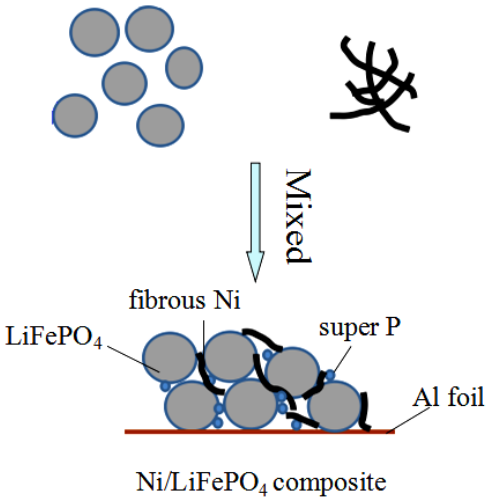

Figure 1. Schematic representation of the electrode from nickel fibers/$LiFePO_4$ composites

2.2. Cell assembly and characterization

The electrochemical performances were tested on 2025-type coin cells with metallic Li foil as the anode. The cathodes were fabricated by a slurry coating process. First, the cathode slurry consisting of 80wt% composite material, 10wt% of conductive carbon black and 10wt% polyvinylidene fluoride (PVDF) were dispersed in N-methylpyrrolidinone (NMP). The nickel fibers loading of the composition of nickel fibers/$LiFePO_4$ in the electrodes were 0wt%, 1wt%, 5wt%, 10wt%, 20wt%, and 30wt%, respectively. Hereafter the corresponding electrodes are denoted as $LiFePO_4$/Ni-0, $LiFePO_4$/Ni-1, $LiFePO_4$/Ni-5, $LiFePO_4$/Ni-10, $LiFePO_4$/Ni-20, and $LiFePO_4$/Ni-30, respectively. Then, the composite slurry was uniformly coated on an aluminum foil current collector and then dried in a vacuum oven at 60ºC overnight. Each electrode was cut into a wafer with diameter of 12 mm and contained about 1.5 mg of active material. The cathode and anode electrodes were separated by celgard 2400 polypropylene (PP) film and Li foil was used as the counter electrode. The electrolyte was a 1 mol L^{-1} lithium hexafluorophosphate ($LiPF_6$) solution dissolved in ethylene carbonate (EC), dimethyl carbonate (DMC) and ethyl methyl carbonate (EMC) (EC: DMC: EMC =1: 1: 1, by v/v ratio). Testing cells were assembled in an argon-filled glove box and were galvanostatically charged/discharged at different current densities between 2.5 and 3.8 V (vs Li/Li^+) using a CT2001A cell test instrument (LAND model, Wuhan RAMBO testing equipment, Co. Ltd.). The cyclic voltammograms (CV) and electrochemical impedance spectroscopy (EIS) measurements were conducted with a VMP2 electrochemical workstation (DHS Instruments Co. Ltd.). The EIS was measured in the frequency range of 0.1 Hz ~100 kHz, while the disturbance amplitude was 10 mV. All the electrochemical properties of the samples were tested at 25ºC.

3. RESULTS AND DISCUSSION

Fig.2 shows the XRD patterns of the nickel fibers, $LiFePO_4$ and nickel fibers/$LiFePO_4$ composites. From Fig.2, it can be observed that the diffraction peaks of nickel fibers and pristine

$LiFePO_4$ are totally consistent with the pure cubic phase of nickel (JCPDS No.04-0850) and orthorhombic $LiFePO_4$ (JCPDS No.40-4199), respectively. Meanwhile, calculated by the Scherrer's equation[21], the average crystallite size of the nickel fibers was determined as 25.85 nm, that of $LiFePO_4$ is 16.72 nm. The main diffraction peaks of the Ni/$LiFePO_4$ composites consist of cubic nickel and orthorhombic $LiFePO_4$ phases, and the peak positions exhibit no obvious change. These results indicate that the composite is just a physical combination of Ni fibers and $LiFePO_4$, no new phase or chemical reaction emerged during the synthesis process.

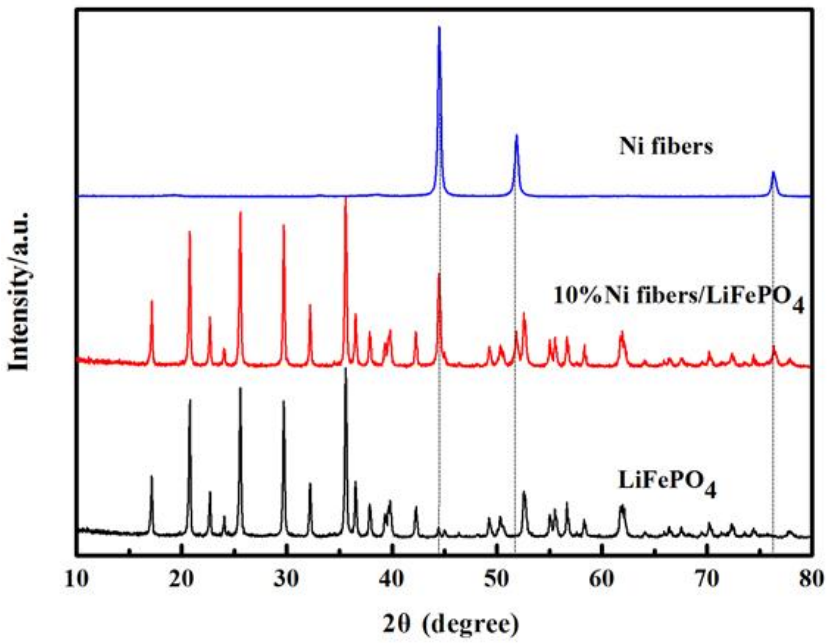

Figure 2. XRD patterns of nickel fibers, $LiFePO_4$, and nickel fibers/$LiFePO_4$ composites

The morphologies of nickel fibers, pure $LiFePO_4$ powders and the nickel fiber/$LiFePO_4$ composite electrode were shown in Fig.3a~c. Fig.3(a) shows that the nickel fibers have 2~5um in length and 0.1~0.5μm in diameter. This kind of fiber has porous structure with specific surface area of 25.8m^2/g, could be in favor of the combination between $LiFePO_4$, additives and current collector surface, and enhance the electron conduction ability of the whole $LiFePO_4$ electrode during charge/discharge process. Fig.3(b) shows the morphology of pure $LiFePO_4$ powders from hydrothermal and post-treatment. From Fig.3(b), it can be seen that the $LiFePO_4$ powders with some soft agglomeration have a particle size less than 1μm. After grinded, the nickel fibers/$LiFePO_4$ composites were uniformly mixed with finer nickel fibers and $LiFePO_4$ particles.

The SEM images of the nickel fibers/$LiFePO_4$ composite electrodes with 10wt% and 20wt% Ni fibers are displayed in Fig. 3 d ~ g, respectively. Though the fiber dispersion in nickel fibers/$LiFePO_4$ composites could remain uniform up to 30 wt%, it seems that there exists an optimal adding amount so as not to increase the difficulty of slurry mixing and the electrode ununiformity. In this experiment, the optimal adding amount of nickel fibers is not more than 10% as shown in Fig.3d and e, the electrode

looks very smooth and compact. Whereas beyond this limit, as shown in Fig.3e, the slurry mixing began to have a little difficult, and the electrode surface became rougher and the adhesion between particles became weak probably due to the increased porosity. The elemental analysis of an electrode fracture surface as shown in Fig.3h displays the elements of P, Fe, O, and Ni, consistent with nickel fibers/$LiFePO_4$ composites.

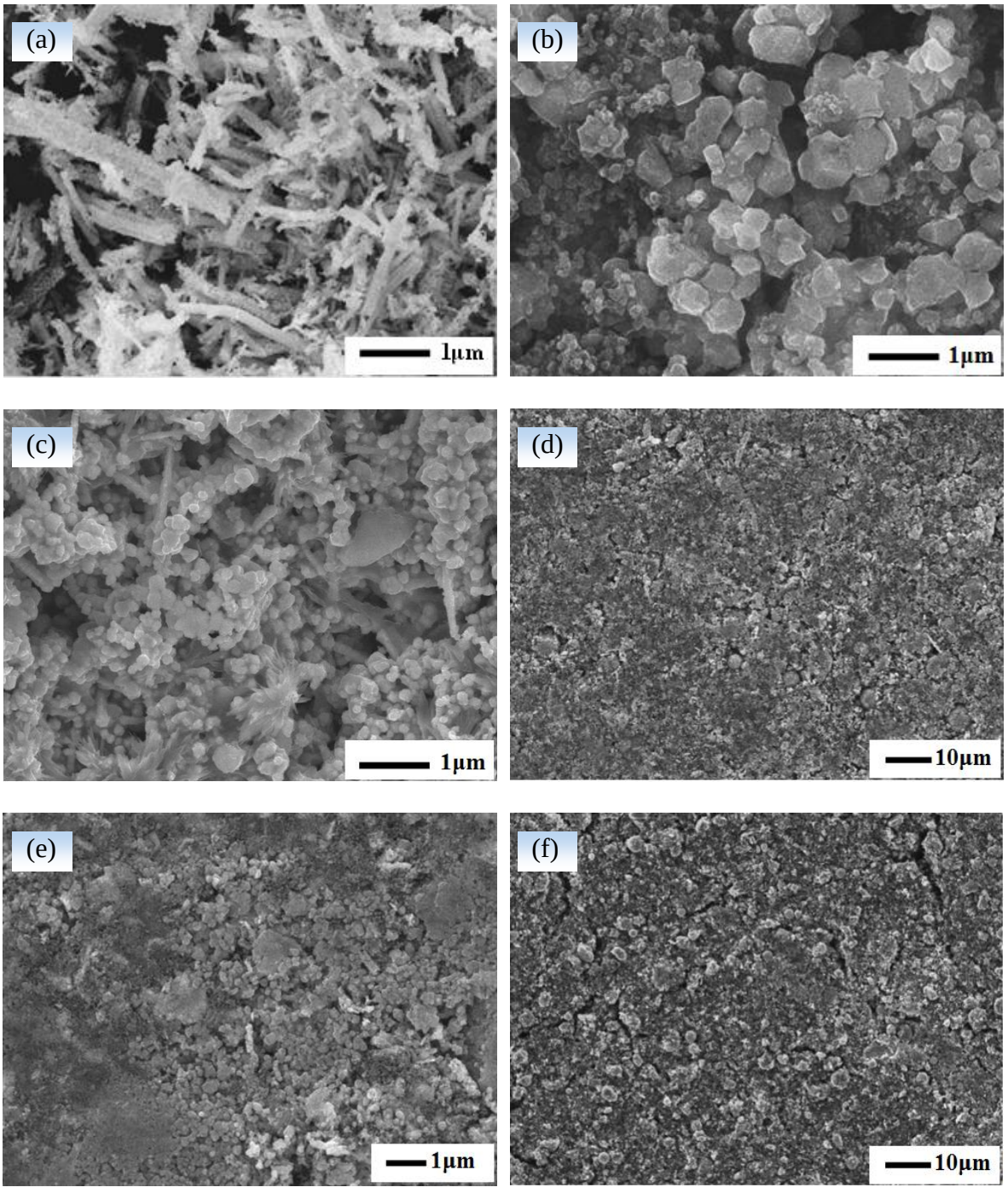

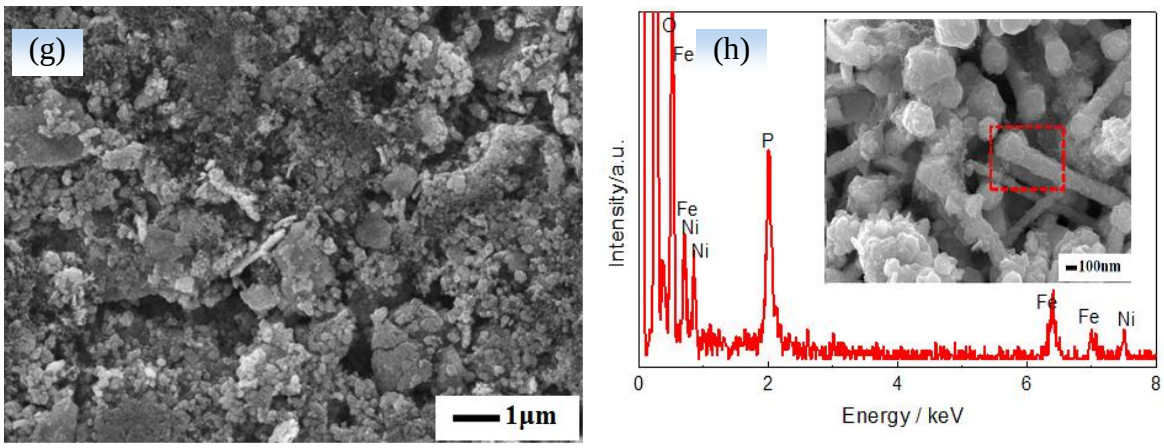

Figure 3. SEM images of (a) nickel fibers; (b) $LiFePO_4$ powders; (c) $LiFePO_4$/Ni-10 composite; (d) and (e) surface of $LiFePO_4$/Ni-10 electrode; (f) and (g) surface of $LiFePO_4$/Ni-20 electrode, and (h) energy-dispersive X-ray spectroscopy of $LiFePO_4$/Ni-20 electrode fracture surface

The effects of nickel fibers on the electrochemical performance of $LiFePO_4$ electrode were analyzed firstly by galvanostatic charge/discharge test. Rate performances of all samples are displayed in Fig.4. It can be seen that all the cells exhibit a tendency to decrease with the rise of current density, but electrodes fabricated from Ni/$LiFePO_4$ composite as lithium-ion battery cathode exhibit better rate performance compared with pristine $LiFePO_4$ at high C. Particularly, the $LiFePO_4$/Ni-10 composite cathode exhibits stable capacity at each step with mean discharge capacity of 150, 134, 129, 103, and 85 mAh g^{-1} at rates of 0.1C, 0.5C, 1C, 3C and 5C, respectively. When the rate is turned back to 1C, a discharge capacity of 122.7 mAh g^{-1}, about 98.3% of the initial capacity at 1C is recovered. While the pristine $LiFePO_4$ electrode exhibits a rapid fading of capacity from 150 mAh g^{-1} to about 60 mAh g^{-1} with the current density increase from 0.1C to 5C.

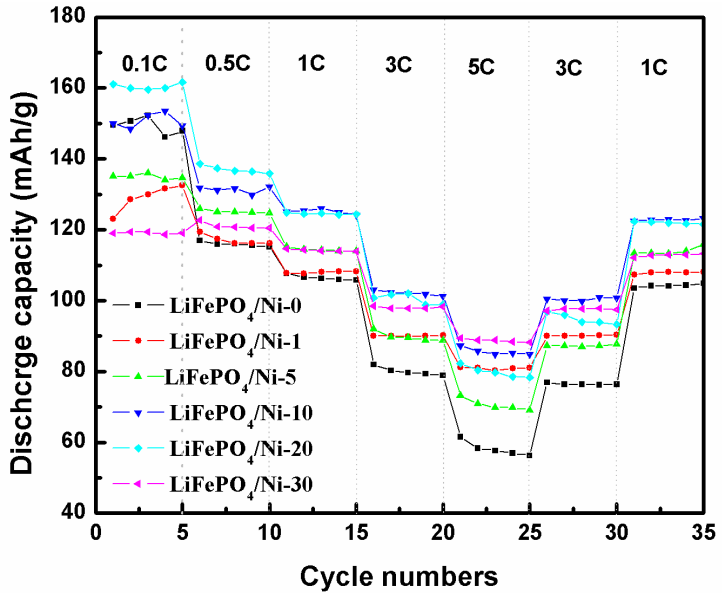

Figure 4. Rate performance of composite electrodes with different fiber content

Meanwhile, it can be found from Fig.5 that the electrodes fabricated from nickel fiber /$LiFePO_4$ composites also exhibit better cyclability compared with pristine $LiFePO_4$. The electrode with 10wt% nickel fibers ($LiFePO_4$/Ni-10) has initial discharge capacity of 131.1 mAh g^{-1} at 1C, and the discharge capacity still has 119.8 mAh g^{-1} after 100 cycles, whereas pristine $LiFePO_4$ can deliver only 108.2 mAh g^{-1} at 1C and retention capacity of 100.9 mAh g^{-1} after 100 cycles.

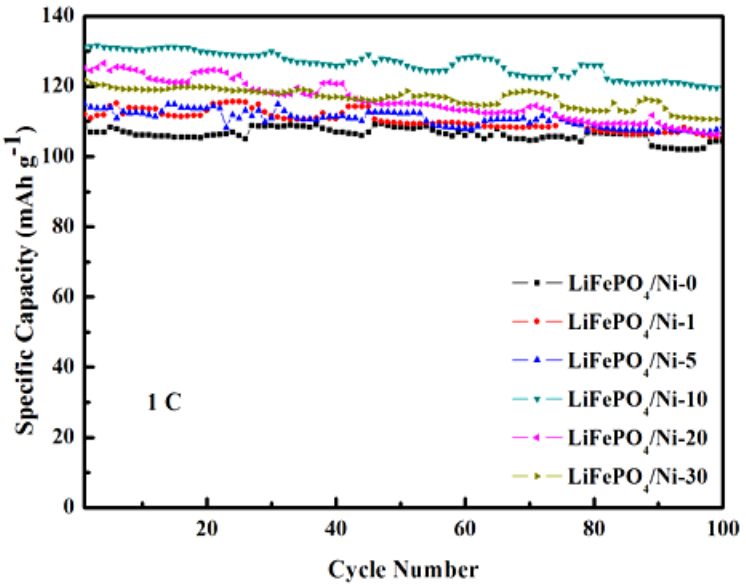

Figure 5. Cyclability performance of composite electrodes with different fiber content at 1C

To reveal the underlying mechanism of enhanced electrochemical performance for $LiFePO_4$/Ni-10, the impedance spectroscopy and cyclic voltammetry properties were measured respectively. Fig.6 shows the cyclic voltammetry characteristics of all the samples at a low scan rate of 0.1 mV s^{-1}. It can be seen that a pair of oxidation and reduction peaks between 2.8 and 4.1 V are observed from all the samples, corresponding to the charge/discharge reaction of the Fe^{2+}/Fe^{3+} redox couple. And the midpoint between the two peaks corresponds to the redox potential of the working electrode, which is equivalent to the charge/discharge platform[22, 23, 24]. Meanwhile, the CV curves also display that compared with pristine $LiFePO_4$, the oxidation and reduction peaks become sharper and the potential intervals decrease with the increase of nickel fiber loading in the composite electrodes. It is known that the smaller separation between redox peaks appearing in $LiFePO_4$ electrodes indicates an enhanced reversible behavior for the redox reaction and the improved diffusion rate of lithium ions [14, 23, 25]. Therefore, this phenomenon illustrates that the redox reaction can be enhanced due to the improved electrical conductivity and decreased polarization with the addition of high conductive nickel fibers. This result is consistent with the EIS analysis as shown in Fig.7. It can be clearly seen that the electrodes of $LiFePO_4$ with nickel fiber additives exhibit more rapid charge-transfer behavior than the pristine $LiFePO_4$. However, when the adding amount of nickel fiber is more than 10wt%, the symmetry of the redox peaks becomes worse, illustrating that the reversibility of redox reaction gets into worse[17, 23, 25], accordingly, the EIS also shows the impedance began to

enlarge with more than 10wt% nickel fibers, which may be related with the worse electrode structure such as more porous and rough surface. Therefore, considering the peak strength and the symmetry of the redox peaks and EIS results, the $LiFePO_4$/Ni-10 composite electrode could have the best redox kinetics.

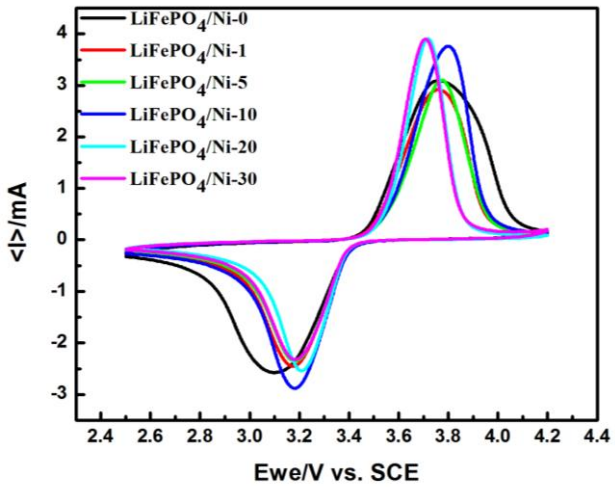

Figure 6. CV curves of composite electrodes with different fiber content

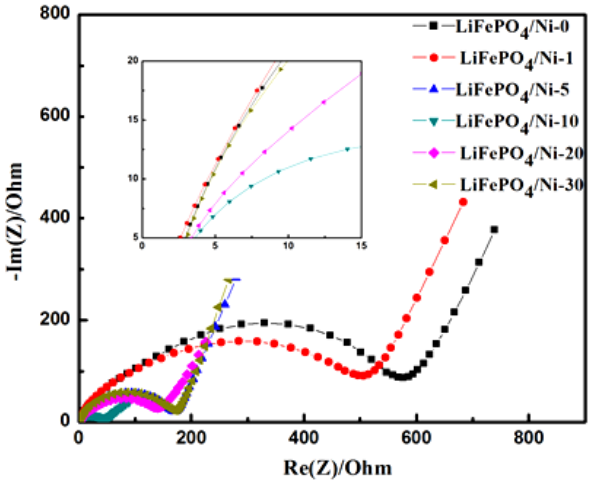

Figure 7. EIS spectra of composite electrodes with different fiber content

4. CONCLUSIONS

Nickel fiber/$LiFePO_4$ composites were prepared by a simple mixing process of $LiFePO_4$ powders and porous nickel fibers. Highly conductive Ni additive enhanced the electronic conductivity of $LiFePO_4$ electrode. Electrode fabricated from Ni/$LiFePO_4$ composite exhibits better electrochemical performance compared with pristine $LiFePO_4$. The electrode with optimal fiber content of 10wt% has a best redox kinetics and possesses an excellent rate capability of 85 mAh g^{-1} at 5C and good cyclability

with initial discharge capacity of 131.1 mAh g^{-1} at 1C, and the retention capacity of 119.8 mAh g^{-1} after 100 cycles.

ACKNOWLEDGEMENTS
This work was supported by the National Natural Science Foundation of China (51274106, 51474113, 51474037), the Science and Technology Support Program of Jiangsu Province of China (BE2013071, BE2014850), the Natural Science Research Program of Jiangsu Province Higher Education of China (grant No. 14KJB430010), the Jiangsu Province's Postgraduate Cultivation and Innovation Project of China (SJZZ15-0131).

Reference

1. A. K. Padhi, K. S. Nanjundaswamy, J. B. Goodenough, *J. Electrochem. Soc*., 144 (1997) 1188.
2. A. Yamada, S. C. Chung, K. Hinokuma, *J. Electrochem. Soc*., 148 (2001) A224.
3. G. X. Wang, H. Liu, J. Liu, S. Z. Qiao, G. M. Lu, P. Munro, H. Ahn, *Adv. Mater*., 22 (2010) 4944.
4. K. Saravanan, M.V. Reddy, P. Balaya, H. Gong, B.V.R. Chowdari, J. J. Vittal , *J. Mater. Chem*., 19 (2009) 605.
5. H. M. Xie, R. S. Wang, J.R. Ying, L.Y. Zhang, A. F. Jalbout, H.Y. Yu, G.L. Yang, X. M. Pan, Z.M. Su, *Adv. Mater*., 18 (2006) 2609.
6. L.Q. Sun, M. J. Li, R.H. Cui, H. M. Xie, R. S. Wang, *J. Phy. Chem. C* , 114 (2010) 3297.
7. H. Huang, S. C. Yin, L.F. Nazar, *Electrochem. Solid-State Lett*., 4 (2001) A170.
8. Z. H. Chen, J. R. Dahn, *J. Electrochem. Soc*., 149 (2002) A1184.
9. B. L. Ellis, W.R.M. Makahnouk, Y. Makimura, K. Toghill, L.F. Nazar, *Nat. Mater*., 6 (2007) 749.
10. C. M. Julien, A. Mauger, K. Zaghib, *J. Mater. Chem.* , 21 (2011) 9955.
11. X. F. Bian , Q. Fu , C. G. Qiu , X. F.Bie , F.Du , Y. H.Wang , Y. Q. Zhang , H. L. Qiu , G. Chen , Y.J.Wei, *Mater. Chem. Phy*., 56 (2015) 69.
12. F. Fathollahi, M. Javanbakht, H. Omidvar, M. Ghaemi, *J. Alloys Compd.*, 627 (2015) 146–152.
13. G. L.Wang , Z. P. Ma , G. J. Shao, L. X. Kong , W. M. Gao, *J. Power Sources* , 291 (2015) 209.
14. S. Ahn , Y. Kim, K. J. Kim, T.H. Kim, H. Lee, M. H. Kim, *J. Power Sources*, 81–82 (1999) 896.
15. X.Y. Lang, L. Zhang, T. Fujita, Y. Ding, M.W. Chen. *J. Power Sources*, 197 (2012) 325.
16. C. Hou, X. Y. Lang, G. F.Han, Y. Q. Li, L. Zhao, Z. Wen, Y.F. Zhu, M. Zhao, J. C. Li, J. S. Lian , Q. Jiang. *Sci. Rep.*, 3 (2013) 2878.
17. H. Tang, S. S. Yao, M. X. Jing, X. Wu, J. L. Hou, X. Y. Qian, D. W. Rao, X. Q. Shen, X. M. Xi, K.S. Xiao, *Electrochim. Acta*, 176 (2015) 442.
18. Y. L. Yao, C. F. Zhang, J. Zhan, F. H. Ding, J. H. Wu, *Trans. Nonferrous Met. Soc. China*, 23 (2013) 3456.
19. J. Zhan, D. F. Zhou, C. F. Zhang, *Trans. Nonferrous Met. Soc. China*, 21 (2011) 544.
20. L.Y. Zhang, Y. F. Tang , Z. Q. Liu , H. N. Huang, Y. Z. Fang , F. Q. Huang , *J. Alloys Compd*., 627 (2015) 132.
21. B.D. Culity, Addision-Weley, London, 1978.
22. K.S. Park, S. B. Schougaard, J. B. Goodenough, *Adv.Mater.*, 19 (2007) 848 .
23. A.K. Padhi, K. S. Nanjundaswamy, C. Masquelier, S. Okada, J.B. Goodenough, *J. Electrochem. Soc*., 144 (1997) 1609.
24. S. T. Myung, Y. Hitoshi, Y. K. Sun, *J. Mater. Chem*., 21 (2011) 9891.
25. X. F. Li, D. M. Luo, X. Zhang, Z. Zhang, *J. Power Sources*, 291(2015)75-84.